On the distribution and function of synaptic clusters

Romain Cazé[1], **Amanda Foust**[1], **Claudia Clopath**[1], **Simon R. Schultz**[1]

[1]Center for Neurotechnology and Dept. of Bioengineering, Imperial College London, South Kensington, London SW7 2AZ, UK

Keywords: Dendrites, Synaptic clustering, Synaptic integration

Abstract

Local non-linearities in dendrites render neuronal output dependent on the spatial distribution of synapses. Previous models predicted that a neuron is more likely to fire when synaptic activity is clustered in space, and some experimental studies have observed synapses activating in clusters. Other studies, however, have revealed that synapses can also uniformly activate across dendrites without apparent spatial bias. In order to reconcile these two sets of observations, we develop a multi-compartment model that: (i) shows how clustered synapses can form and distribute throughout available compartments, and (ii) responds, subsequent to learning, most saliently to uniformly distributed

synaptic activity. We measure co-activation probability to show that cluster formation and distribution depend on correlated activity within input ensembles that impinge on multiple compartments, each operating a local unsupervised, Hebbian learning rule. Clustered synapses evolve in response to long-term, learned input ensembles, heightening a neuron's sensitivity to scattered "novel" inputs. As a result of the proposed learning rule, clustered inputs correspond to familiar pre-learned stimuli, while scattered inputs depolarize the cell for novel, unlearned stimuli. Our model reconciles seemingly conflicting experimental evidence, and suggests how clustered and scattered synapses together could underlie single neuron discrimination between familiar and novel inputs.

1 Introduction

Synaptic contacts distribute non-uniformly on neurons (Druckmann et al., 2014; Rah et al., 2015), particularly on pyramidal neurons, as foreseen by previous theoretical studies (Mel, 1992; Poirazi and Mel, 2001; Poirazi et al., 2003). Because dendrites, including even passive dendrites (Koch et al., 1982), are non-linear, the relative position of synapses exerts a salient influence on the neuronal input-output function. Non-uniform synaptic spatial distribution can enhance the computational capacity of single neurons. In particular, non-uniform synaptic configurations allow neurons to compute linearly inseparable functions (Zador et al., 1993; Caze et al., 2012), enhance auditory coincidence detection (Agmon-Snir et al., 1998), help compute binocular disparity (Archie and Mel, 2000), as well as contributing to whisker directional tuning in the barrel cortex (Lavzin et al., 2012). Theoretical studies predicted the existence of synaptic clusters

(Mel, 1992; Poirazi and Mel, 2001; Poirazi et al., 2003). Importantly, nearby synapses on dendrites co-activate more often than spatially separated synapses.

Experimental results have provided, however, seemingly conflicting evidence. On the one hand, Takahashi et al. observed clustering of active synapses during spontaneous activity in adult rats (Takahashi et al., 2012). Kleindienst et al. also reported synaptic clustering in organotypic slices from neonatal rats during development (Kleindienst et al., 2011). Moreover, synaptic clustering can evolve during sensory experience (Makino and Malinow, 2011). On the other hand, uniform synaptic activation has been reported several times (Varga et al., 2011; Chen et al., 2011; Jia et al., 2010). These observations from multiple sensory modalities including touch (Varga et al., 2011), vision (Jia et al., 2010), and hearing (Chen et al., 2011) all demonstrate uniform synaptic activation during sensory episodes.

How can neural activity form and distribute synaptic clusters? How can we reconcile uniform synaptic activation with the presence of synaptic clusters? In order to address these seemingly contradictory lines of evidence, we developed a multi-compartment model. We show that a unique instance of this model can display both clustered and scattered synaptic activity depending on the context, thus reconciling experimental data. Our model suggests that familiar stimuli evoke clustered activity whereas novel stimuli evoke scattered activity.

Materials and Methods

Controlling correlation in ensembles of Poisson processes

The input spike trains are modeled as ensembles of correlated Poisson processes (Brette, 2009). Each process is the sum of an independent process with a frequency $f(1-c)$ and of a process common to the ensemble with a frequency $f \times c$ (f in hertz and $c \in [0, 1]$ without units). Fig. 1A shows examples of spike trains that were generated using this method. In this study we used seven ensembles each composed of 100 neurons, firing at a mean rate of 10 Hz with 80% of their spikes correlated within the ensemble. These spike trains lasted 40s, made up of 4000 bins of 10ms. During the last 20s of each spike train, we rotated all of the 100 ensemble neurons by 50 (see Fig.4B).

A multi-compartment binary neuron model.

We computed the mean somatic depolarization in time bins of 10ms using our multi-compartment model. This computation has two steps, as in (Poirazi et al., 2003). For each bin, the binary inputs x_i first sum linearly in each compartment, given a local set of weights $w_{i,j}$ for the compartment j. A uniform synaptic architecture is presented on Fig 1B. Secondly, this sum is normalized by the maximal possible activity within the compartment, non-linearly resulting in $v_i = \sum_j D_i(w_{i,j}x_{i,j})$. v_i denotes a local signal that could be interpreted as either the mean membrane potential or the mean calcium concentration in compartment i. D is a function with a threshold θ at which v jumps to 1. Then all the resulting v are linearly summed at the soma to determine whether it fires or not: $y = S\big(\sum_i v_i\big)$, where S is a Heaviside function with threshold

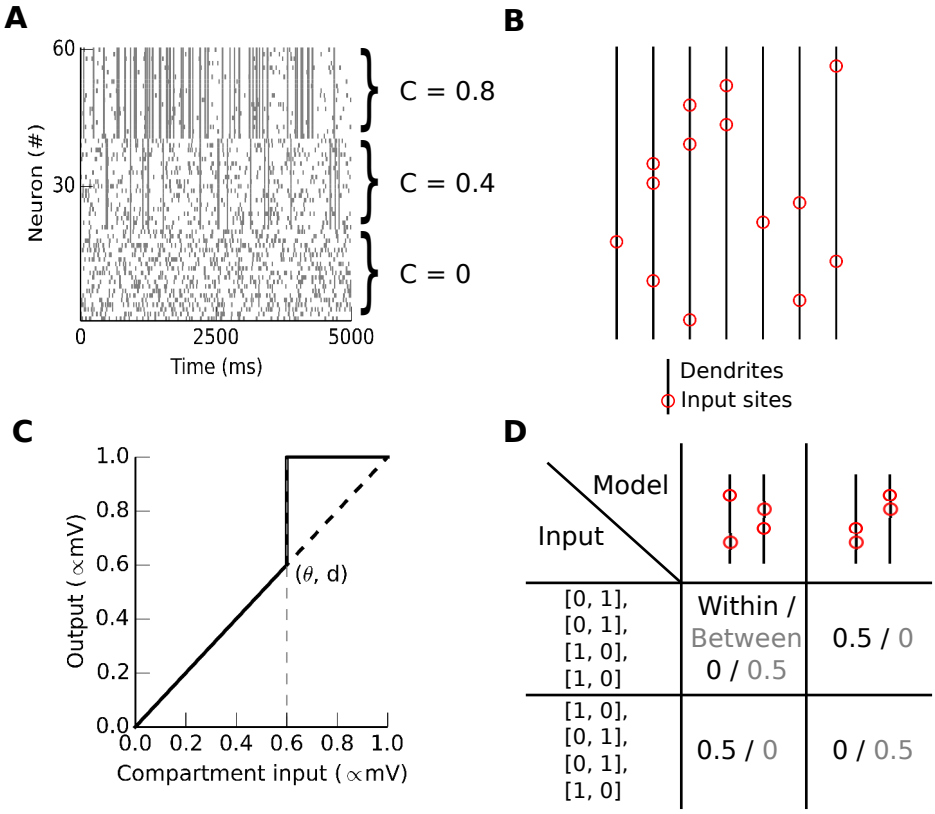

Figure 1: **Correlated inputs and a multi-compartmental model to study the spatial distribution of synapses**. **A**. Raster plot showing the activity of three ensembles each with a different level of internal correlation. Neurons 0-19, 20-41 and 42-61 have 0, 0.4 and 0.8 correlation respectively. **B** The input sites (red circles) are where the connections are most numerous on dendritic compartments (black vertical lines). **C** The dendritic compartment non-linear transfer function. The input is the weighted sum of the presynaptic activity, and the output of this function is transmitted to the soma. **D** Table showing the co-activation probability for two synaptic architectures and two sets of input spikes.

$\Theta = 0.2$. This value for Θ means that 20% of the compartments need to reach their maximum depolarization to elicit a somatic spike. We used a somatic threshold of 0.2,

a dendritic threshold of 0.2 and synaptic weights bounded between 0.01 and 1 modeling only excitatory synapses.

In contrast with more detailed biophysical models, our model lacks temporal integration, and its compartments process inputs independently. We have however previously demonstrated that this model would nonetheless yield the same conclusions if we were to relax these assumptions (Caze et al., 2013). This simplicity enables formal and in-depth analyses that would be cumbersome with a detailed biophysical model.

A local learning rule and horizontal normalization.

The learning rule uses the local signal v_j of the j^{th} compartment to compute the weight change $\Delta w_{i,j} = \alpha(2x_i - 1)v_j$ where $\alpha = 0.1$ is the learning rate. Consistent with experimental data, the learning rule depends on a local signal in the dendrites. Plasticity depending only on dendritic spikes and independent of somatic spikes has been observed repeatedly (Feldman, 2012; Mehta, 2004; Kim et al., 2015).

In each time bin, the synaptic weights arising from a given source are normalized by the total synaptic weight from this source. This is to account for the limited number of synapses per afferent (Branco and Staras, 2009). We introduced this normalization to foster an optimal distribution of synaptic clusters on dendrites (compare movie S1 and S3 respectively with and without normalization), and to focus on the spatial distribution of synapses rather than the total synaptic strength from an afferent.

Co-activation probability.

We define the co-activation probability of a pair of synapses as the fraction of bins in which these synapses co-activate, analogous to previous experimental studies (Kleindienst et al., 2011; Takahashi et al., 2012). The co-activation probability depends on two distinct variables: the input spike train and the set of synaptic weight values (see Fig. 1D).

To compute the co-activation probability, we first select the compartment bearing the highest weight for a given input, indicated by empty circles in subsequent figures. We then either replay the input spike train, or replay the seven input vectors corresponding to the seven ensembles. In the later case, each input vector corresponds to the activation of one ensemble. We then select every possible pair of synapses, and classify each as occurring either ”within” or ”between” compartments. The co-activation probability is the number of times a pair is active, over the total number of activations of a synapse in this pair.

Results

Correlated inputs distribute synapses in clusters

Correlated inputs evoke synaptic clusters that distribute evenly on dendrites. First we examine a neuron receiving inputs from two ensembles and featuring two compartments as in Fig. 2. We describe the evolution of the two mean synaptic weights, one per ensemble, using a 2D vector field. Importantly, this 2D vector field demonstrates only two stable point: (0,1) and (1,0) in all conditions. Hence synapses either from the first

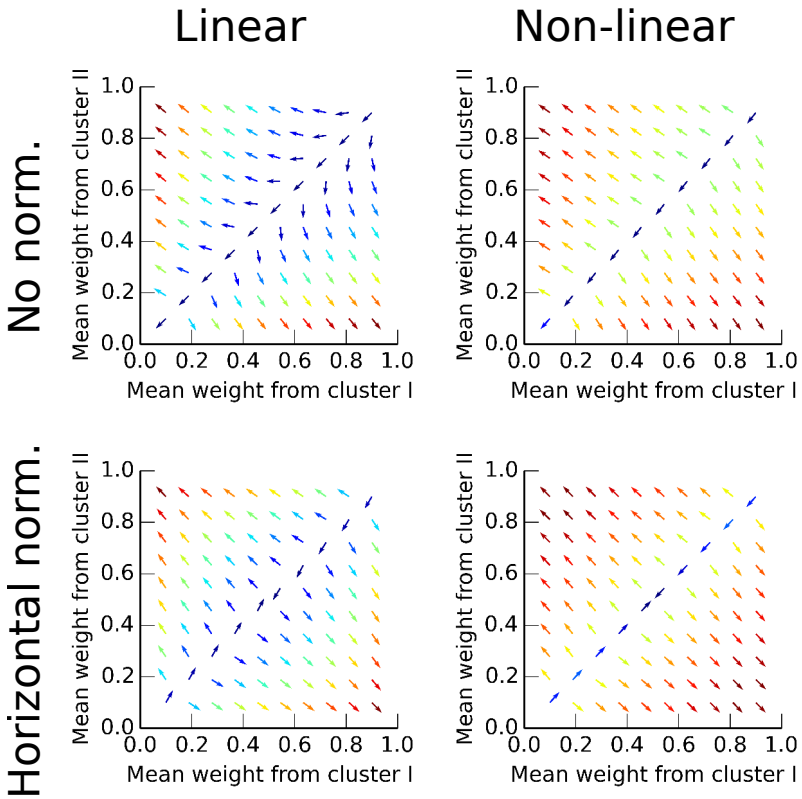

Figure 2: **Vector fields showing the evolution of the mean synaptic weight per cluster**. The arrow's origin is the mean synaptic weight value. It points in the direction of the average evolution of these means and is color-coded given the intensity of this movement (blue:low, red:high). Note that only (0,1) and (1,0) stay stable in the four situations, with or without normalization and with linear ($theta = 1$, $d = 1$) or non-linear summation in compartments ($theta = 0.5$, $d = 0.5$).

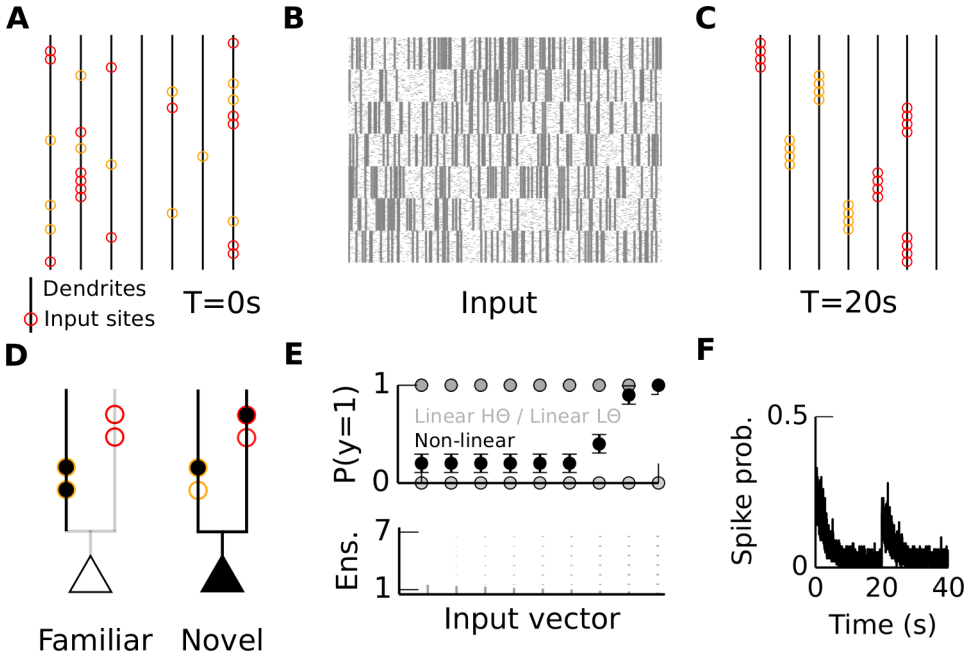

Figure 3: **Correlated inputs generate synaptic clusters that enable detection of stimuli deviating from typical input statistics.** **A**. A naive model where vertical lines are dendrites and circles are the most probable synaptic sites, is exposed to **B** synaptic inputs organized in correlated ensembles. **C** It results in a specific (and different for each ensemble) spatial distribution of active synapses (color coded, red-yellow flip depending on the ensemble origin). **D** Neuron's response (triangle) for two types of presynaptic activity (clustered:familiar and scattered:novel); activity is color-coded (white:inactive / black:active). **E** Mean spiking probability for 9 different input vectors (700 axons). **F** Mean spiking probability for each time bin for non-linear models ($n = 100$). In the linear case this would have been a flat line because of horizontal normalization (see Methods).

or the second ensemble grow together to form a cluster (Fig. 2 upper left, "linear"). Saturation within a compartment when it activates more than 50% ($(\theta = 0.5, d = 0.5)$) sharpens the vector field toward the stable points (Fig. 2 upper right, "non-linear"). Interestingly, horizontal normalization, in which each input has a constant total synaptic weight, guarantees that a cluster forms only once. Without horizontal normalization, the same ensemble can form clusters on multiple compartments.

We scaled up our implementation to show that seven ensembles, made of 100 neurons each, can form evenly distributed synaptic clusters (Fig. 3). Before receiving any input, synapses distribute randomly on the neuron (Fig. 3A). After receiving inputs organized in seven correlated ensembles (Fig. 3B), seven synaptic clusters form on the neuron with one cluster per ensemble (Fig. 3C). Movie S1 illustrates that horizontal normalization fosters an even cluster distribution. Without normalization, synaptic clusters form, but the same cluster can occur multiple times as illustrated by Movie S3.

Non-linear integration in dendrites can render a neuron sensitive to scattered synaptic activation. For low dendritic threshold, a clustered learned input ensemble will trigger a single dendritic spike, whereas a scattered ensemble will trigger many. For a high somatic threshold, a neuron requires multiple dendritic spikes to drive a somatic spike. Because our learning rule gives rise to evenly distributed clusters on a model with non-linear compartments, a novel unlearned stimulus can saliently activate the neuron (Fig 3E).

The sensitivity to the spatial distribution of inputs gives rise to an important functional role. We measured the response of two types of neuron models integrating their inputs either non-linearly or linearly (100 instance of each). In the linear case, the neu-

ron responds to all inputs equally regardless of the input spatial distribution. There are seven ensembles each made of 100 axons. Each axon makes a contact with a total synaptic weight always equal to one (see Methods Horizontal normalization). Therefore, for a somatic threshold larger than 100/700, a linear neuron fires for all input vectors, and for a threshold lower than 100/700, a linear neuron stays silent for all input vectors (Fig 3E grey lines). In the non-linear case, however, the firing probability changes (Fig 3F black line). If the input vector corresponds to the activation of all axons within a learned ensemble, then the neuron remains silent. If the vector corresponds to the activation of axons distributed among different ensembles, then the neuron fires. In summary, a neuron integrating its input non-linearly can signal an unfamiliar input deviating from the learned set of ensembles. This is illustrated by the mean firing probability plotted as a function of time (Fig 3F) where we present a new ensemble set at $t = 20s$.

In summary, we have demonstrated that synaptic clusters evenly distribute on a multi-compartment model under horizontal normalisation. We then demonstrated a potential functional role for these learned synaptic clusters. Next we examine how changes in input statistics affect the distribution of synaptic clusters.

Changes in input statistics can reshape synaptic clusters

We started from a model displaying synaptic clusters ($t = 20s$ on Fig 4A), and then exposed it to inputs organized into a new ensemble set between $t = 20s$ and $t = 40s$ (Fig 4B). Notably, this reshaped the spatial distribution of synapses to reflect the new ensembles set (Fig 4C). It occurs because the new set of ensembles reshapes the

vectors field defining the synaptic weights evolution. There used to be seven stable points with a precise position , e.g. (1, 0, 0, 0, 0, 0, 0). The number of stable points remained constant, but their position shifted according to the rotation of the ensemble set (rotated by $n = 50$ neurons). Therefore, long-lasting changes to input statistics reshape the synaptic architecture. Contrary to classical unsupervised algorithms, this learning occurs continuously in our model. These changes can be visualized in Movie S3 and S4, respectively, with or without horizontal normalization.

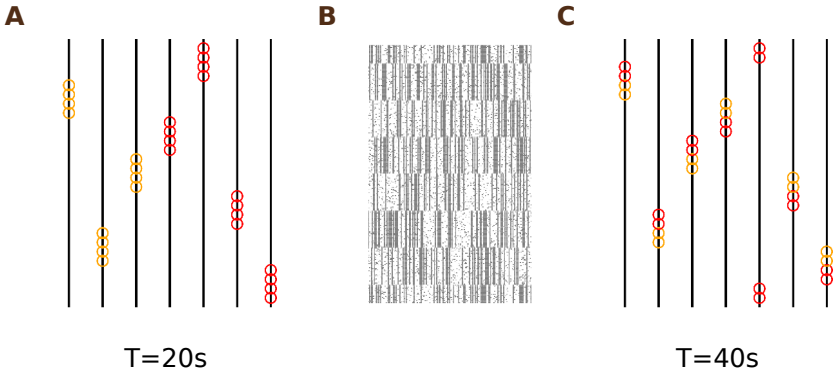

Figure 4: **Changes in input statistics can reshape synaptic clusters. A** Synaptic architecture at $t = 20s$ and after exposing the model **B** to a new ensemble set **C** resulting in a new synaptic architecture $t = 40s$.

Co-activation probability quantifies the distribution and formation of synaptic clusters

We show that the formation of synaptic clusters in our model recapitulates co-activation probabilities measured in experiments (Kleindienst et al., 2011; Takahashi et al., 2012) (Fig. 5A-B). The co-activation probability is the fraction of time bins in which both

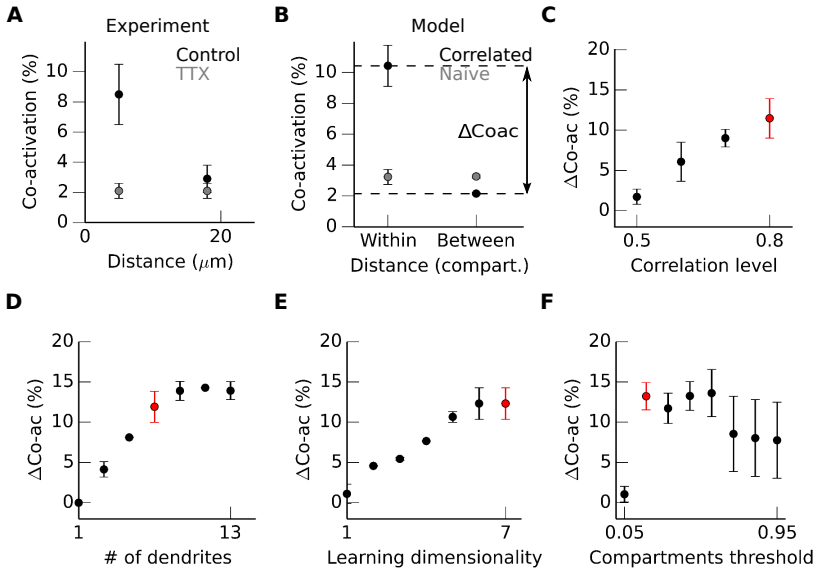

Figure 5: **Co-activation probability quantifies synaptic cluster distribution**. **A**. Measurements of spines co-activation probability in hippocampal slices, control situation and cultureed within a TTX environment, washed out during measurement (replotted from Kleindienst et al 2011). **B**. Co-activation probability obtained in silico (see methods). Difference of co-activation "between" and "within" dendritic compartments, depending on the input correlation. ΔCoac is the difference between within and between co-activation probabilities. The mean ΔCoac probabilities (dots) are obtained after five iterations of the model. We fix the value of all other parameters (red dot) while varying each in turn. We quantify the effect of **C** Input correlation, **D** Compartmentalization, **E** Learning dimensionality and **F** the dendritic threshold.

synapses activate (see Methods for examples). Kleindienst et al. reported that co-activation probability depends on the distance between spines (Fig. 5A). Similarly in our model, co-activation probability is higher for "within" compared to "between" compartments. ΔCo-ac is the difference between these two cases. Moreover, ΔCo-ac becomes null in the absence of previous correlated activity as reported experimentally (compare "TTX" in Fig. 5A and "naive" in Fig. 5B).

We use co-activation probability to investigate which parameters influence the distribution of synaptic clusters. We identified four parameters with which ΔCoac varies: (A) the input correlation (B) the number of compartments (C) the number of learning parameters (dimensionality of learning) and (D) non-linear summation within a compartment (four panels in Fig.5). While varying each parameter in turn, we kept all other parameters constant.

Correlation within an ensemble of axons must be sufficiently high to generate synaptic clustering. We found that in our model only input correlation greater or equal to 60% achieved a ΔCoac larger than 5% (Fig.5C). The more correlated the input, the higher the ΔCoac observed. We infer that correlations are necessary for the formation of synaptic clusters. Moreover, the formation of multiple synaptic cluster requires multiple compartments. Even in an integrate and fire model, synapses cluster in response to correlated inputs, and a single cluster forms. However, ΔCoac is always zero in that case, as all synapses target only one compartment. For example, in the case of seven input ensembles, three or more compartments are required for a ΔCoac larger than 5% (Fig.5D).

Even in a model with multiple compartments, it is possible to use a single v (e.g.

membrane voltage or calcium concentration) that results from synaptic integration. In this case, v applies to all compartments and the learning dimensionality is one. Alternately, one can use multiple vs each assigned to distinct sets of compartments. For seven input ensembles, we found that three or more distinct vs are required for a ΔCoac larger than 5% (Fig.5E).

Finally, we studied the influence of the dendritic threshold on cluster distribution. Unlike the three other parameters, ΔCoac reaches its highest value in a large range (here between 0.1 and 0.4). For a high threshold (0.7 and above) integration is quasi-linear because synaptic activity does not reach the compartment's threshold. Synaptic clusters can form even in this case (Fig.5F). Local non-linear integration is not necessary for synaptic cluster formation, but it guarantees their even distribution across compartments and novelty detection capacity.

Discussion

The theoretical framework that we have proposed unifies two apparently contradictory sets of experimental observations. Correlated inputs and a multi-compartment model endowed with a learning rule based on a local signal Clopath et al. (2010) can generate synaptic clusters. We have shown that a single instance of this model can display both clustered and scattered synaptic activation, as observed in recent experimental studies (Kleindienst et al., 2011; Takahashi et al., 2012; Chen et al., 2011; Jia et al., 2010). We use co-activation probability to demonstrate that the learning rule needs a sufficient number of parameters, and the model needs a large enough number of compartments,

to display evenly distributed clusters. Furthermore, local non-linearities enable neurons to signal novel stimuli, and could play a crucial role in stimulus selectivity.

We set a high somatic threshold requiring multiple dendritic spikes to trigger a somatic spike. In this case, the neuron detects novel stimuli and stays silent for familiar stimuli. This case has been observed *in vivo*, where multiple dendritic spikes are required to trigger an action potential (Jia et al., 2014). Alternatively, a single dendritic spike might suffice to generate an action potential. Wu and Mel studied this scenario and described how dendrites could boost memory capacity at the network level (Wu and Mel, 2009). In this dual case, the neuron will fire for familiar stimuli and stay silent for novel stimuli and requires supra-linear summation in dendrites (Caze et al., 2012). Both cluster and scatter sensitivities could prevail depending on the cell type and the brain area.

The learning algorithm presented here is unsupervised, but it differs significantly from previous examples of this type of algorithm (Legenstein and Maass, 2011). Our work differs in two aspects. First, we introduced horizontal normalization, in which an input makes a constant number of synapses on a post-synaptic neuron. This was initially introduced for biological realism as each neuron makes a limited number of synapses (Branco and Staras, 2009). This normalization also avoids synaptic cluster repetition in multiple compartments of the post-synaptic neuron. In this case, the detection of novel stimuli would be compromised. Second, we do not split inputs into training and test sets. This renders our neuron model more realistic and enables it to continuously adapt to a changing sensory environment.

This computational work yields two immediate predictions: (1) A given neuron

can display both clustered and scattered synaptic activity. This could be tested by *in vivo* two-photon imaging of the same neuron across periods of both spontaneous and sensory-evoked activity. (2) An ensemble forms a single cluster only when an axon has a constant number of pre-synaptic contacts. Time lapse imaging of synapses from a single afferent could test this prediction.

In conclusion, we have proposed a learning mechanism to organize the distribution of synapses in space. This mechanism could possibly underpin the emergence of stimulus selectivity underlying a wide range of neural computations.

Acknowledgments

The author would like to thank Mark Humphries and Lyle-Borg Graham for their comments on earlier versions of the manuscript, and Jacopo Bono for proof reading of this manuscript.

References

Agmon-Snir, H., Carr, C., and Rinzel, J. (1998). The role of dendrites in auditory coincidence detection. *Nature*, 393(6682):268–272.

Archie, K. A. and Mel, B. W. (2000). A model for intradendritic computation of binocular disparity. *Nature Neuroscience*, 3(1):54–63.

Branco, T. and Staras, K. (2009). The probability of neurotransmitter release: variability and feedback control at single synapses. *Nature*, 10(may):373–383.

Brette, R. (2009). Generation of correlated spike trains. *Neural computation*, 21(1):188–215.

Caze, R., Humphries, M., and Gutkin, B. (2012). Spiking and saturating dendrites differentially expand single neuron computation capacity . *NIPS*, pages 1–9.

Caze, R. D., Humphries, M., and Gutkin, B. (2013). Passive Dendrites Enable Single Neurons to Compute Linearly Non-separable Functions. 9(2).

Chen, X., Leischner, U., Rochefort, N. L. N., Nelken, I., and Konnerth, A. (2011). Functional mapping of single spines in cortical neurons in vivo. *Nature*, 475(7357):501–5.

Clopath, C., Büsing, L., Vasilaki, E., and Gerstner, W. (2010). Connectivity reflects coding: a model of voltage-based STDP with homeostasis. *Nature neuroscience*, 13(3):344–52.

Druckmann, S., Feng, L., Lee, B., Yook, C., Zhao, T., Magee, J. C., and Kim, J. (2014). Structured Synaptic Connectivity between Hippocampal Regions. *Neuron*, 81(3):629–640.

Feldman, D. E. (2012). The Spike-Timing Dependence of Plasticity. *Neuron*, 75(4):556–571.

Jia, H., Rochefort, N. L., Chen, X., and Konnerth, A. (2010). Dendritic organization of sensory input to cortical neurons in vivo. *Nature*, 464(7293):1307–1312.

Jia, H., Varga, Z., Sakmann, B., and Konnerth, A. (2014). Linear integration of spine Ca2+ signals in layer 4 cortical neurons in vivo. *Proceedings of the National Academy of Sciences of the United States of America*, 111(25):9277–82.

Kim, Y., Hsu, C.-L., Cembrowski, M. S., Mensh, B. D., and Spruston, N. (2015). Dendritic sodium spikes are required for long-term potentiation at distal synapses on hippocampal pyramidal neurons. *eLife*, 4(August):1–30.

Kleindienst, T., Winnubst, J., Roth-Alpermann, C., Bonhoeffer, T., and Lohmann, C. (2011). Activity-Dependent Clustering of Functional Synaptic Inputs on Developing Hippocampal Dendrites. *Neuron*, 72(6):1012–1024.

Koch, C., Poggio, T., and Torres, V. (1982). Retinal ganglion cells: a functional interpretation of dendritic morphology. *Phil. Trans. R. So. Lond. B*, 298(1090):227–263.

Lavzin, M., Rapoport, S., Polsky, A., Garion, L., and Schiller, J. (2012). Nonlinear dendritic processing determines angular tuning of barrel cortex neurons in vivo. *Nature*, 490(7420):397–401.

Legenstein, R. and Maass, W. (2011). Branch-Specific Plasticity Enables Self-Organization of Nonlinear Computation in Single Neurons. *Journal of Neuroscience*, 31(30):10787–10802.

Makino, H. and Malinow, R. (2011). Compartmentalized versus Global Synaptic Plasticity on Dendrites Controlled by Experience. *Neuron*, 72(6):1001–1011.

Mehta, M. R. (2004). Cooperative LTP can map memory sequences on dendritic branches. *Trends in neurosciences*, 27(2):69–71.

Mel, B. W. (1992). NMDA-based pattern discrimination in a modeled cortical neuron. *Neural Computation*, 517:502–517.

Poirazi, P., Brannon, T., and Mel, B. (2003). Pyramidal neuron as two-layer neural network. *Neuron*, 37(6):989–999.

Poirazi, P. and Mel, B. W. (2001). Impact of active dendrites and structural plasticity on the memory capacity of neural tissue. *Neuron*, 29(3):779–796.

Rah, J.-C., Feng, L., Druckmann, S., Lee, H., and Kim, J. (2015). From a meso- to micro-scale connectome: array tomography and mGRASP. *Frontiers in Neuroanatomy*, 9(June):1–12.

Takahashi, N., Kitamura, K., Matsuo, N., Mayford, M., Kano, M., Matsuki, N., and Ikegaya, Y. (2012). Locally Synchronized Synaptic Inputs. *Science*, 335(6066):353–356.

Varga, Z., Jia, H., Sakmann, B., and Konnerth, A. (2011). Dendritic coding of multiple sensory inputs in single cortical neurons in vivo. *Proceedings of the National Academy of Sciences*, 108(37):15420–15425.

Wu, X. E. and Mel, B. W. (2009). Capacity-enhancing synaptic learning rules in a medial temporal lobe online learning model. *Neuron*, 62(1):31–41.

Zador, A. A. M., Claiborne, B., Brown, T. T. H., and Clairborne, B. J. (1993). Nonlinear pattern separation in single hippocampal neurons with active dendritic membrane. *Advances in neural information processing systems*, pages 51–51.

Supporting Information

S1 Video

Formation and distribution of synaptic clusters. Activity is color-coded (white:inactive / black:active). The diameter of a circle relates to the number of spines on an input site. Triangle describes somatic activity.

S2 Video

Redistribution of synaptic clusters.

S3 Video

Formation of synaptic clusters without horizontal normalization.

S4 Video

Redistribution of synaptic clusters without horizontal normalization.

Software and code availability

. We used Python v2.7, Numpy v1.3 and Matplotlib v1.4.0 to code, process and display the result of all our simulations. This code is available on a git repository (link to be supplied after acceptance of this manuscript, we uploaded this code for review with a README file).